

Supplement of Atmos. Chem. Phys., 20, 9563–9579, 2020
<https://doi.org/10.5194/acp-20-9563-2020-supplement>
© Author(s) 2020. This work is distributed under
the Creative Commons Attribution 4.0 License.



Supplement of

Oxygenated products formed from OH-initiated reactions of trimethylbenzene: autoxidation and accretion

Yuwei Wang et al.

Correspondence to: Lin Wang (lin_wang@fudan.edu.cn)

The copyright of individual parts of the supplement might differ from the CC BY 4.0 License.

Table S1 Relative abundance of the C9 and C18 oxidation products formed from TMB oxidation (Exp. #1-3 in Table 1), as measured by Nitrate CI-API-TOF. The percentages mean the relative intensity of this compound family to the total signals of detected C9 and C18 products with correction of the relative transmission efficiency of Nitrate CI-API-TOF obtained by the previously reported depletion method (Heinritzi et al., 2016). All of these products, except for C₉H₁₄O₅ that was detected in the 1,2,4-TMB and 1,2,3-TMB experiments, have more than 6 oxygen atoms, which meet the definition of HOMs from Bianchi et al (2019).

Compound Family	1,3,5-TMB	1,2,4-TMB	1,2,3-TMB
C ₉ H ₁₂ O ₆₋₁₁	1.9 %	6.6 %	7.5 %
C ₉ H ₁₄ O ₅₋₁₁	5.9 %	10.2 %	18.3 %
C ₉ H ₁₆ O ₆₋₁₀	5.7 %	9.6 %	11.8 %
C ₁₈ H ₂₄ O ₈₋₁₃	3.2 %	4.9 %	4.0 %
C ₁₈ H ₂₆ O ₈₋₁₅	33.4 %	23.1 %	26.5 %
C ₁₈ H ₂₈ O ₉₋₁₅	44.9 %	39.0 %	26.9 %
C ₁₈ H ₃₀ O ₁₂₋₁₅	5.1 %	6.6 %	5.0 %

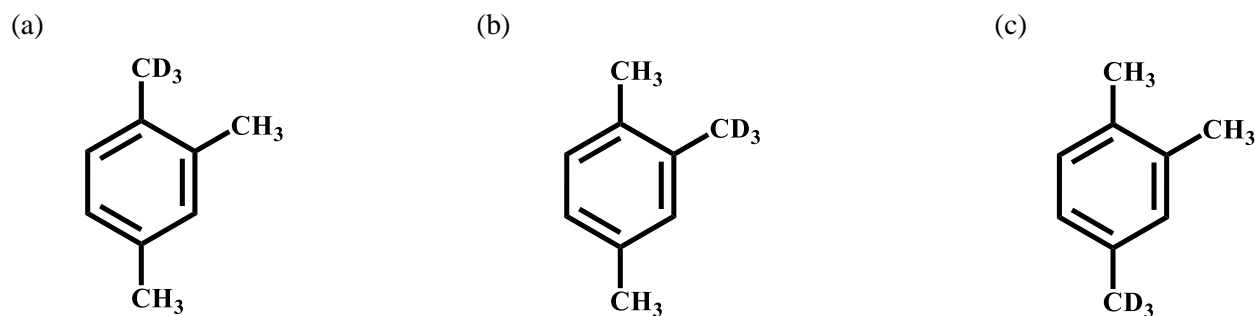


Figure S1. Molecular structure of three partially deuterated precursors. (a) 1,2,4-(1-methyl-D3)-TMB; (b) 1,2,4-(2-methyl-D3)-TMB; and (c) 1,2,4-(4-methyl-D3)-TMB.

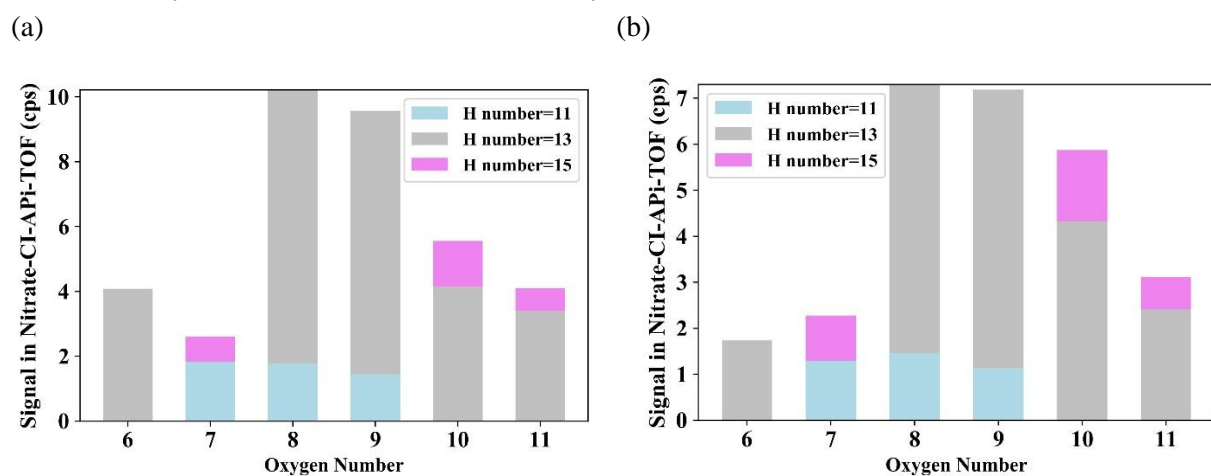


Figure S2. (a) Distribution of $C_9H_xN_1O_y$ formed from 1,2,4-TMB under low NO_x conditions, as detected by Nitrate CI-APi-TOF; and (b) Distribution of $C_9H_xN_1O_y$ formed from 1,2,4-TMB under higher NO_x conditions, as detected by Nitrate CI-APi-TOF.

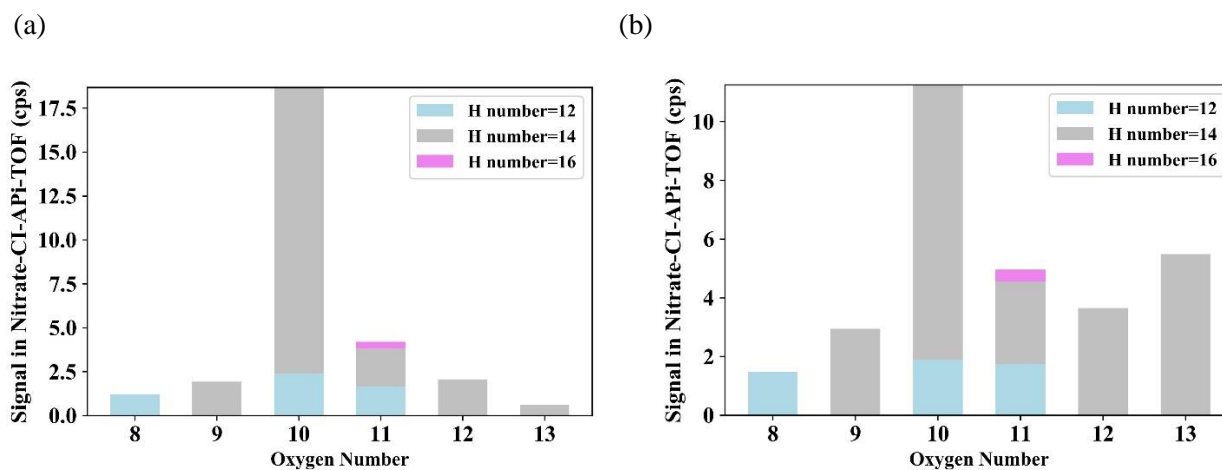


Figure S3. (a) Distribution of $C_9H_xN_2O_y$ formed from 1,2,4-TMB under low NO_x conditions, as detected by Nitrate CI-APi-TOF; and (b) Distribution of $C_9H_xN_2O_y$ formed from 1,2,4-TMB under higher NO_x conditions, as detected by Nitrate CI-APi-TOF.

Section S1:

PAM_chem_v8 is a model developed in conjunction with the PAM, which includes the chemistry of photolysis of oxygen, water vapor, and other trace gases by the primary wavelengths in mercury lamps (254 nm and 185 nm) (Lambe et al., 2017; Li et al., 2015; Peng et al., 2015). Simplified VOC and RO_2 chemistry are also included, but the first-generation stabilized products and the second-generation organic radical products do not react further in the model.

Fig S4 shows the modelled concentration profiles of different oxidants and 1,3,5-TMB with an irradiance of 1.64×10^{15} ph cm^{-2} s by 254 nm lamps. The initial concentrations of O_3 ($[O_3]$) (1.2 ppm) and 1,3,5-TMB ($[1,3,5-TMB]$) were measured before turning on the 254 nm lamps. $[O_3]$ and $[1,3,5-TMB]$, at an 80 s residence time were also measured. The modelled $[O_3]$ is 20% lower than the measured value whereas modelled $[1,3,5-TMB]$ is very close (4% higher) to the measured one, which shows the reliability of this model.

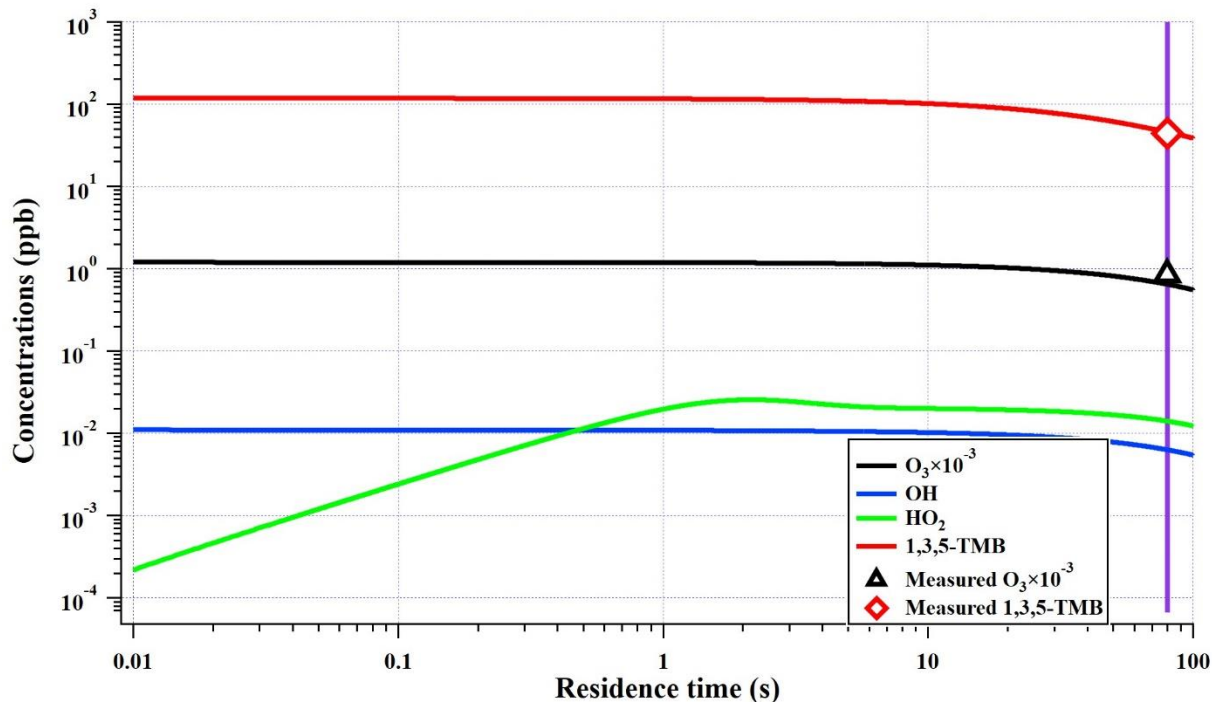
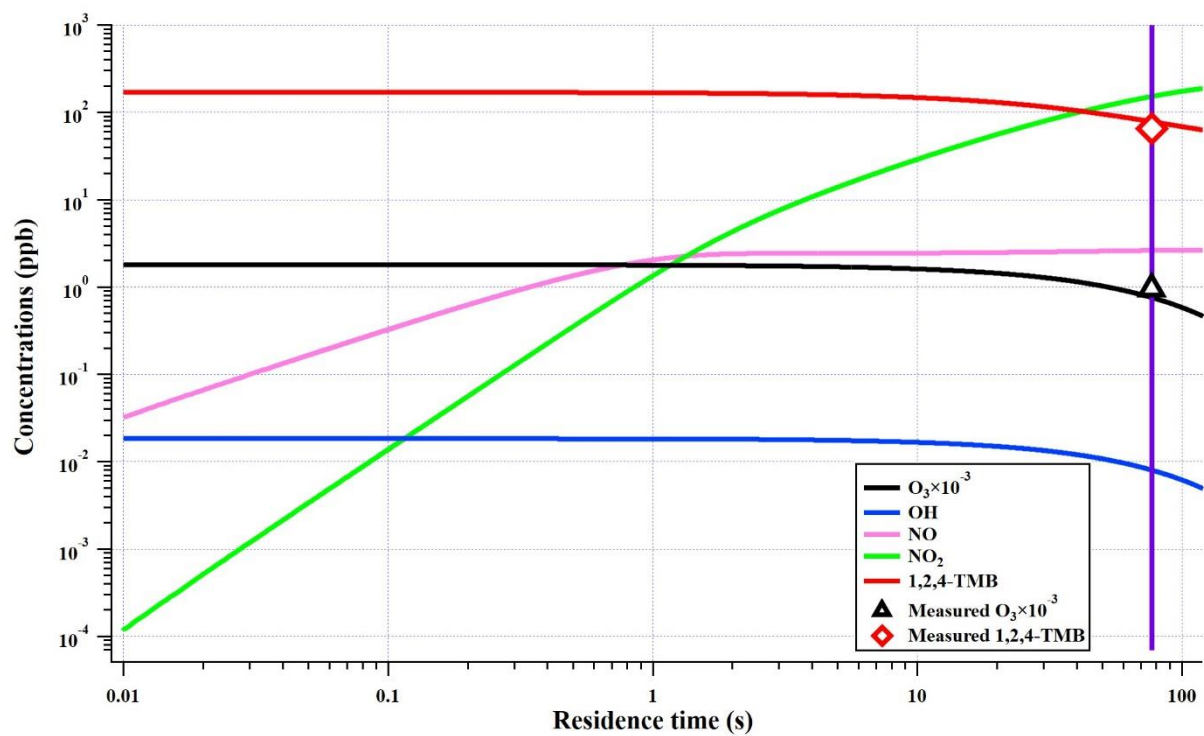


Figure S4. Concentration profiles of different oxidants and 1,3,5-TMB outputted by PAM_chem_v8 under the settings of Exp. #2. Initial $[O_3]$ and [1,3,5-TMB] are 1.2 ppm and 118 ppb, respectively, which were used as input of the model. The measured $[O_3]$ and [1,3,5-TMB] at the exit of OFR are shown by a triangle and a diamond, respectively. Input of irradiance of 254 nm lamps, I_{254} , is 1.64×10^{15} ph cm^{-2} s, which was measured with a photodiode in the OFR. The vertical purple line represents a residence time of 80 s.

Figure S5 shows the modelled profiles of the major oxidants, NO_x , and the precursor under the settings of Exp. #7 and Exp. #8 in Table 1. In the low NO_x experiment, the modelled $[O_3]$ is 20% lower than the measured value at the exit of OFR whereas the modelled [1,2,4-TMB] is 19% higher than the measured one. In the higher NO_x experiment, the modelled $[O_3]$ is 3% higher than the measured value whereas the modelled [1,2,4-TMB] is 23% higher than the measured one.

(a)



(b)

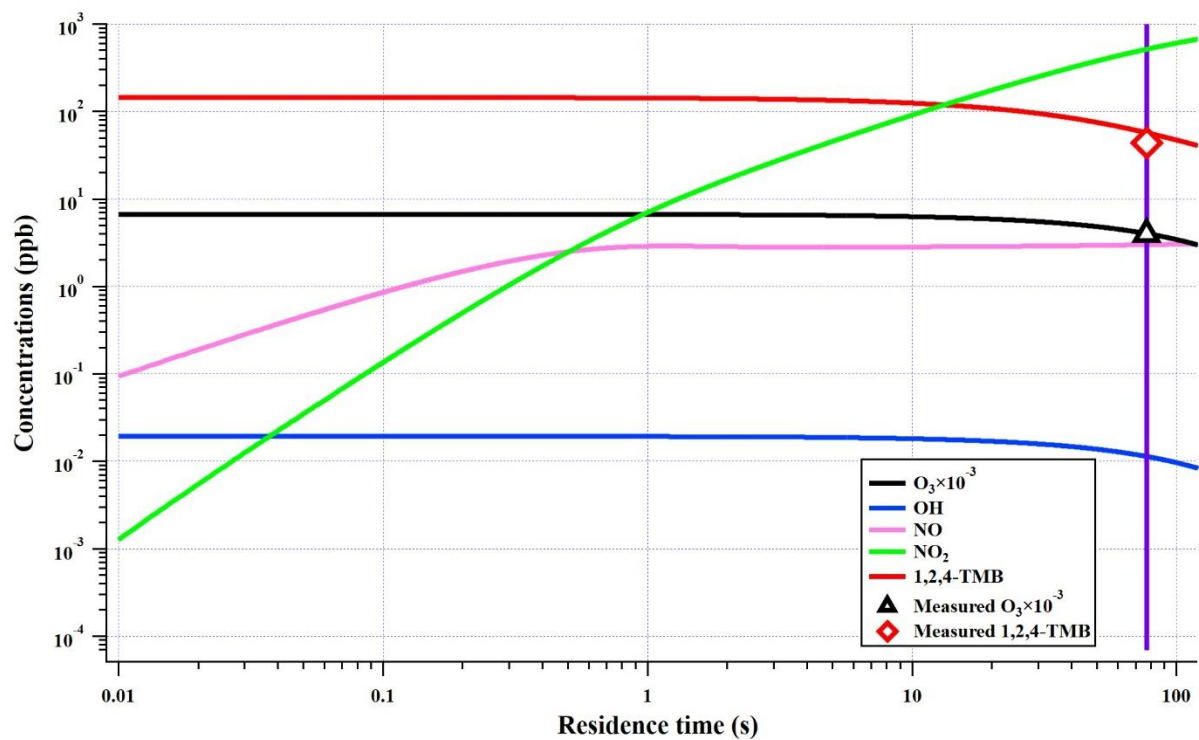


Figure S5. Modelled profiles by PAM_chem_v8 of different oxidants, NO_x and the precursor under the settings of (a) low NO_x experiment (initial $[O_3] = 1.8$ ppm, initial $[1,2,4-TMB] = 170$ ppb, and irradiance

of 254 nm Lamps = 2.0×10^{15} ph cm^{-2} s) and (b) higher NO_x experiment (initial $[\text{O}_3] = 6.7$ ppm, initial $[\text{1,2,4-TMB}] = 145$ ppb, and irradiance of 254 nm Lamps = 1.28×10^{15} ph cm^{-2} s). The measured $[\text{O}_3]$ and $[\text{1,2,4-TMB}]$ at the exit of OFR are shown by a triangle and a diamond in the plot. The vertical purple line represents a residence time of 77.3 s.

References

- Bianchi, F., Kurtén, T., Riva, M., Mohr, C., Rissanen, M. P., Roldin, P., Berndt, T., Crounse, J. D., Wennberg, P. O., Mentel, T. F., Wildt, J., Junninen, H., Jokinen, T., Kulmala, M., Worsnop, D. R., Thornton, J. A., Donahue, N., Kjaergaard, H. G. and Ehn, M.: Highly Oxygenated Organic Molecules (HOM) from Gas-Phase Autoxidation Involving Peroxy Radicals: A Key Contributor to Atmospheric Aerosol, *Chem. Rev.*, 119(6), 3472–3509, doi:10.1021/acs.chemrev.8b00395, 2019.
- Heinritzi, M., Simon, M., Steiner, G., Wagner, A. C., Kürten, A., Hansel, A. and Curtius, J.: Characterization of the mass-dependent transmission efficiency of a CIMS, *Atmos. Meas. Tech.*, 9(4), 1449–1460, doi:10.5194/amt-9-1449-2016, 2016.
- Lambe, A., Massoli, P., Zhang, X., Canagaratna, M., Nowak, J., Daube, C., Yan, C., Nie, W., Onasch, T., Jayne, J., Kolb, C., Davidovits, P., Worsnop, D. and Brune, W.: Controlled nitric oxide production via $O(1D) + N_2O$ reactions for use in oxidation flow reactor studies, *Atmos. Meas. Tech.*, 10(6), 2283–2298, doi:10.5194/amt-10-2283-2017, 2017.
- Li, R., Palm, B. B., Ortega, A. M., Hlywiak, J., Hu, W., Peng, Z., Day, D. A., Knote, C., Brune, W. H., De Gouw, J. A. and Jimenez, J. L.: Modeling the radical chemistry in an oxidation flow reactor: Radical formation and recycling, sensitivities, and the OH exposure estimation equation, *J. Phys. Chem. A*, 119(19), 4418–4432, doi:10.1021/jp509534k, 2015.
- Peng, Z., Day, D. A., Stark, H., Li, R., Lee-Taylor, J., Palm, B. B., Brune, W. H. and Jimenez, J. L.: HO x radical chemistry in oxidation flow reactors with low-pressure mercury lamps systematically examined by modeling, *Atmos. Meas. Tech.*, 8, 4863–4890, doi:10.5194/amt-8-4863-2015, 2015.